Published in final edited form as:
*Nature*. 2007 May 10; 447(7141): 218–221. doi:10.1038/nature05740.

# The carboxy terminus of NBS1 is required for induction of apoptosis by the MRE11 complex

**Travis H. Stracker**[1], **Monica Morales**[1], **Suzana S. Couto**[2], **Hussein Hussein**[1], and **John H. J. Petrini**[1,3]

[1] Molecular Biology and Genetics, Sloan-Kettering Institute, New York, New York 10021, USA

[2] Pathology and Laboratory Medicine, Memorial Sloan-Kettering Cancer Center, New York, New York 10021, USA

[3] Weill-Cornell Graduate School of Medical Science, New York, New York 10021, USA

## Abstract

The MRE11 complex (MRE11, RAD50 and NBS1) and the ataxia-telangiectasia mutated (ATM) kinase function in the same DNA damage response pathway to effect cell cycle checkpoint activation and apoptosis[1–3]. The functional interaction between the MRE11 complex and ATM has been proposed to require a conserved C-terminal domain of NBS1 for recruitment of ATM to sites of DNA damage[4,5]. Human Nijmegen breakage syndrome (NBS) cells and those derived from multiple mouse models of NBS express a hypomorphic *NBS1* allele that exhibits impaired ATM activity despite having an intact C-terminal domain[3,6–11]. This indicates that the NBS1 C terminus is not sufficient for ATM function. We derived $Nbs1^{\Delta C/\Delta C}$ mice in which the C-terminal ATM interaction domain is deleted. $Nbs1^{\Delta C/\Delta C}$ cells exhibit intra-S-phase checkpoint defects, but are otherwise indistinguishable from wild-type cells with respect to other checkpoint functions, ionizing radiation sensitivity and chromosome stability. However, multiple tissues of $Nbs1^{\Delta C/\Delta C}$ mice showed a severe apoptotic defect, comparable to that of ATM- or CHK2-deficient animals. Analysis of p53 transcriptional targets and ATM substrates showed that, in contrast to the phenotype of $Chk2^{-/-}$ mice, $NBS1^{\Delta C}$ does not impair the induction of proapoptotic genes. Instead, the defects observed in $Nbs1^{\Delta C/\Delta C}$ result from impaired phosphorylation of ATM targets including SMC1 and the proapoptotic factor, BID.

To address the role of the conserved C-terminal domain of NBS1, homologous recombination was used to delete exon 15 of the *Nbs1* (also known as *Nbn*) gene (Supplementary Fig. 1). Splicing from exon 14 to 16 in the ensuing allele, hereafter designated $Nbs1^{\Delta C}$, results in a nonsense mutation. The messenger RNA transcribed from the targeted allele encodes an NBS1 protein that terminates after a non-native isoleucine and lacks the C-terminal 24 amino acids, which include the ATM binding domain (Fig. 1a, b). Western blotting confirmed that a smaller NBS1 protein was produced (Fig. 1c) and immunoprecipitation with NBS1 antisera demonstrated that the MRE11 complex was intact and present at normal levels in $Nbs1^{\Delta C/\Delta C}$ cells (Fig. 1d). In contrast to cells from NBS

Correspondence and requests for materials should be addressed to J.H.P. (petrinij@mskcc.org).

**Full Methods** and any associated references are available in the online version of the paper at www.nature.com/nature.

Supplementary Information is linked to the online version of the paper at www.nature.com/nature.

**Author Contributions** T.H.S. and J.H.P. conceived the experiments and wrote the paper. T.H.S., M.M., S.S.C., and H.H. performed the experiments.

patients and *Nbs1*$^{\Delta B/\Delta B}$ mice[6,9], the MRE11 complex exhibited normal nuclear localization and ionizing-radiation-induced foci (IRIF)-formation in *Nbs1*$^{\Delta C/\Delta C}$ cells (Supplementary Fig. 2a). *Nbs1*$^{\Delta C/\Delta C}$ mice were viable and born in normal mendelian ratios, and they did not exhibit overt developmental defects.

Unlike *Atm*$^{-/-}$cells, *Nbs1*$^{\Delta C/\Delta C}$ mouse embryo fibroblasts (MEFs) did not senesce prematurely, did not exhibit increased spontaneous chromosome aberrations and were not sensitive to γ-irradiation (Supplementary Fig. 2b, c, and data not shown)[12–14]. *Atm*$^{-/-}$ mice uniformly develop thymic lymphoma from 2 to 8 months of age[12,14]. Whereas 90% of *Atm*$^{-/-}$mice in our colony present with lymphoma by 8 months, none has been observed in *Nbs1*$^{\Delta C/\Delta C}$ mice of the same age (Supplementary Fig. 3a).

*Atm*$^{-/-}$ mice and ATM-deficient cells from ataxia telangiectasia patients are defective in the activation of DNA-damage-dependent checkpoints at the G1/S and G2/M transitions, and within S phase[3,12–14]. Cells established from NBS patients, and from mice that model the *Nbs1*$^{657\Delta 5}$ allele, have normal G1/S checkpoints[15,16], but are defective in the imposition of intra-S-phase and G2/M DNA-damage-dependent checkpoints[9,11,17]. Neither the G1/S nor the G2/M DNA-damage-dependent cell cycle checkpoints were altered in early passage *Nbs1*$^{\Delta C/\Delta C}$ MEFs, indicating that these ATM-dependent checkpoints did not require the NBS1 C terminus (Fig. 2a, b). In contrast, *Nbs1*$^{\Delta C/\Delta C}$ cells exhibited an intra-S-phase checkpoint defect comparable to *Nbs1*$^{\Delta B/\Delta B}$, suppressing DNA synthesis after 10 Gy of ionizing radiation by 36% compared with 51% in wild type (Fig. 2c).

In response to ionizing radiation, ATM phosphorylates SMC1; this event is required for imposition of the intra-S-phase checkpoint[18]. Consistent with the defect observed, SMC1 phosphorylation on ionizing radiation exposure was reduced in *Nbs1*$^{\Delta C/\Delta C}$ cells (Fig. 2d). This did not seem to reflect impaired ATM activation because ATM autophosphorylation (at Ser 1981), an index of ATM activation[19], was unaffected in *Nbs1*$^{\Delta C/\Delta C}$ (Fig. 2e). These data suggest that the NBS1 C-terminal domain governs the access of activated ATM to SMC1, and that impairing this event contributes to the checkpoint defect of *Nbs1*$^{\Delta C/\Delta C}$ cells.

In contrast to the relatively minor impact on cell cycle checkpoint functions, *Nbs1*$^{\Delta C}$ exerted a profound influence on apoptosis. *Rad50*$^{S/S}$ mice, which express the hypermorphic *Rad50*$^{S}$ allele, exhibit ATM-dependent apoptotic attrition of haematopoietic cells, resulting in death from anaemia at 2–3 months of age[2,20]. *Rad50*$^{S/S}$ mice thus provide a uniquely sensitive context to assess ATM function. The onset of age-dependent anaemia in *Rad50*$^{S/S}$ mice was markedly reduced by the presence of even a single *Nbs1*$^{\Delta C}$ allele[2]. *Rad50*$^{S/S}$ *Nbs1*$^{+/\Delta C}$ and *Rad50*$^{S/S}$ *Nbs1*$^{\Delta C/\Delta C}$ mice did not exhibit pathology at 8 months, an age at which 97.5% of *Rad50*$^{S/S}$ mice succumbed to anaemia (Supplementary Fig. 3b)[2,20]. Flow cytometry confirmed that the attrition of B-, T- and myeloid-cell lineages was mitigated in *Rad50*$^{S/S}$ *Nbs1*$^{\Delta C/\Delta C}$ mice (Supplementary Fig. 4). *Rad50*$^{S/S}$ mice also exhibit apoptosis in the semeniferous tubules[20] and the gut epithelium (Fig. 3a). Apoptosis in *Rad50*$^{S/S}$ *Nbs1*$^{\Delta C/\Delta C}$ testes and gut was substantially mitigated, demonstrating that the effect of *Nbs1*$^{\Delta C}$ on apoptosis was not confined to haematopoietic cells (Fig. 3a, and Supplementary Figs 5 and 6).

Having established that *Nbs1*$^{\Delta C}$ impaired apoptotic cellular attrition induced by the *Rad50*$^{S}$ allele, we examined the induction of apoptosis by ionizing radiation. *Nbs1*$^{\Delta C/\Delta C}$ mice were irradiated and thymi were examined by immunohistochemical staining for cleaved caspase-3. Similar to *Atm*$^{-/-}$, thymi from *Nbs1*$^{\Delta C/\Delta C}$ mice showed reduced caspase staining after 10 Gy, indicating an attenuated apoptotic response to ionizing radiation *in vivo* (Fig. 3b).

To obtain a more quantitative view of the apoptotic defect, ionizing-radiation-induced apoptosis was assessed in *Nbs1*$^{\Delta C/\Delta C}$ thymocytes *ex vivo*. Cultured thymocytes were γ-irradiated with 0.5, 1, 2, 4, 6 and 8 Gy, and annexinV-positive cells, indicative of apoptosis, were scored by flow cytometry. At each ionizing radiation dose, apoptosis of *Nbs1*$^{\Delta C/\Delta C}$ thymocytes was reduced (Fig. 3c); the reduction was comparable in magnitude to *Atm*$^{-/-}$ or *Chk2*$^{-/-}$ (also known as *Chek2*$^{-/-}$) thymocytes at 5 Gy (Fig. 3d). This analysis also revealed that the distribution of CD4, CD8 and double-positive thymocytes in *Nbs1*$^{\Delta C/\Delta C}$ was indistinguishable from wild type (Supplementary Fig. 4b); hence, *Nbs1*$^{\Delta C/\Delta C}$ does not phenocopy *Atm*$^{-/-}$ in which thymic differentiation is impaired[14].

If the apoptotic function of ATM were dependent on the NBS1 C terminus, *Nbs1*$^{\Delta C/\Delta C}$ would be epistatic to *Atm* deficiency with respect to its apoptotic defect[4,5]. To test this, we interbred *Nbs1*$^{+/\Delta C}$ and *Atm*$^{+/-}$ mice. Homozygous double mutants were viable and born at the expected mendelian ratios (data not shown). Thymocyte apoptosis in double mutants was comparable to *Atm*$^{-/-}$ or *Nbs1*$^{\Delta C/\Delta C}$, consistent with the interpretation that the apoptotic functions of ATM are largely dependent on the C-terminal domain of NBS1 (Fig. 3d). To determine if CHK2 functioned in the same signalling pathway as ATM and NBS1 in the thymus, we generated *Atm*$^{-/-}$ *Chk2*$^{-/-}$ double-mutant mice. Apoptosis in response to ionizing radiation was as deficient as in cells lacking p53 (Fig. 3d). Hence, p53-dependent apoptosis is regulated in parallel, with CHK2 on one arm and the MRE11 complex and ATM on the other.

p53's influence on apoptosis in the thymus is mediated in part through transcriptional regulation of proapoptotic genes. This aspect of p53 function is dependent on CHK2, and only partially impaired by ATM deficiency[21,22]. To address the mechanistic basis of the *Nbs1*$^{\Delta C/\Delta C}$ apoptotic defect, changes in the levels of *Bax* and *Puma* (also known as *Bbc3*) mRNA were assessed at 8 h post 5 Gy of ionizing radiation using quantitative PCR. The levels of *Bax* and *Puma* mRNA were similar in both *Nbs1*$^{\Delta C/\Delta C}$ and wild-type thymocytes (Fig. 4a). In contrast, cells lacking CHK2 or p53 were almost completely deficient in their induction (Fig. 4a). These data support the view that MRE11-complex-dependent apoptotic induction is largely CHK2-independent, consistent with previous data indicating that NBS1 and CHK2 exert parallel influences on the intra-S-phase checkpoint[23].

Having established that transcriptional regulation was unaffected in *Nbs1*$^{\Delta C/\Delta C}$ mice, we examined ATM substrates. The levels and phosphorylation status of the ATM substrates p53, CHK2 and the apoptotic effector BID were examined after ionizing radiation treatment. The ATM-dependent phosphorylation of BID was markedly reduced in *Nbs1*$^{\Delta C/\Delta C}$ cells (Fig. 4b). This finding is particularly compelling in light of the fact that *Nbs1*$^{\Delta C/\Delta C}$ phenocopies BID deficiency with respect to apoptotic and intra-S-phase checkpoint defects[24,25]. In contrast, no defects in the ATM-dependent and MRE11-complex-dependent hyperphosphorylation of CHK2 was observed in *Nbs1*$^{\Delta C/\Delta C}$ cells (Fig. 4c). Similarly, the phosphorylation and stabilization of p53 after ionizing radiation, which is defective in *Atm*$^{-/-}$ and *Chk2*$^{-/-}$ cells[21,22,26], was normal in *Nbs1*$^{\Delta C/\Delta C}$ (Fig. 4b). These data support a model wherein the MRE11 complex, through the C terminus of NBS1, facilitates access of ATM to substrates that include effectors of apoptosis, and, in which the MRE11 complex and ATM act in parallel to CHK2. An implicit prediction of this model is met: the apoptotic defects of ATM- and CHK2-deficiency are additive (Fig. 3d).

Loss of the NBS1 C terminus exerts a relatively circumscribed effect: NBS1$^{\Delta C}$ does not impair p53 phosphorylation, stabilization or transcriptional responses but reduces the ability of ATM to phosphorylate SMC1 as well as the proapoptotic BID protein. The phenotypic similarities between *Nbs1*$^{\Delta C/\Delta C}$ and *Bid*$^{-/-}$ are consistent with the view that BID is among the major ATM-dependent apoptotic effectors impaired in *Nbs1*$^{\Delta C/\Delta C}$ (refs [24, 25]). The

precise role of BID phosphorylation in apoptosis remains unclear, but our data are consistent with the view that dynamic modification of BID influences apoptosis.

The findings presented support the functional significance of the NBS1 C terminus for ATM activity *in vivo*; however, the specificity of the *Nbs1*$^{\Delta C/\Delta C}$ phenotype clearly demonstrates that ATM recruitment is not mediated solely by the NBS1 C terminus. *In vitro* analyses using purified proteins[27], as well as the phenotypic differences between *Nbs1*$^{\Delta B/\Delta B}$ (lacking the N terminus)[9] and *Nbs1*$^{\Delta C/\Delta C}$ mice, illustrate that ATM makes multiple contacts with members of the MRE11 complex. We propose that ATM signalling (and presumably recruitment) may be mediated by distinct molecular determinants within the MRE11 complex, as well as in other DNA damage sensors and response mediators, and that different outcomes of the ATM–MRE11-complex DNA damage response may be governed by distinct molecular interactions.

## METHODS SUMMARY

### Cellular assays

Ionizing radiation sensitivity, analysis of chromosomal aberrations, G1/S, G2/M, and intra-S-phase checkpoint assays were performed as described[28].

### Immunoblotting, immunoprecipitation and immunofluorescence

Immunoblotting and immunoprecipitations were carried out as described previously[2,29]. For analysis of NBS1 localization, MEFs were fixed in 4% formaldehyde and permeabilized with 0.25% TX-100. For IRIF analysis cells were fixed in 1:1 methanol:acetone 8 h post treatment with 10 Gy of ionizing radiation. Images were captured on a Zeiss Axiovert and imaged with a CCD camera using Volocity (Improvision) and cropped in Photoshop (Adobe).

### Apoptotic analysis

Apoptosis in thymocytes was assessed as previously described[29] at 20 h post ionizing radiation treatment, with the indicated dose. Haematopoietic cell preparation and analysis was performed as described[20].

## Supplementary Material

Refer to Web version on PubMed Central for supplementary material.

## Acknowledgments

We thank N. Copeland, N. Jenkins, and C. Adelman for assistance with recombineering and ES cell culture, J. Theunissen for assistance with checkpoint and apoptotic analysis, G. Oltz and E. Rhuley for AC1 ES cells, Y. Shiloh for anti-ATM (MAT3) antibodies, and Petrini laboratory members for helpful suggestions. T.H.S. was supported by an NRSA fellowship and this work was supported by NIH grants awarded to J.H.P. and the Joel and Joan Smilow Initiative.

## References

1. Stracker TH, Theunissen JW, Morales M, Petrini JH. The Mre11 complex and the metabolism of chromosome breaks: the importance of communicating and holding things together. DNA Repair. 2004; 3:845–854. [PubMed: 15279769]
2. Morales M, et al. The *Rad50*$^{S}$ allele promotes ATM-dependent DNA damage responses and suppresses ATM deficiency: implications for the Mre11 complex as a DNA damage sensor. Genes Dev. 2005; 19:3043–3054. [PubMed: 16357220]

3. Shiloh Y. ATM and related protein kinases: safeguarding genome integrity. Nature Rev Cancer. 2003; 3:155–168. [PubMed: 12612651]
4. You Z, Chahwan C, Bailis J, Hunter T, Russell P. ATM activation and its recruitment to damaged DNA require binding to the C terminus of Nbs1. Mol Cell Biol. 2005; 25:5363–5379. [PubMed: 15964794]
5. Falck J, Coates J, Jackson SP. Conserved modes of recruitment of ATM, ATR and DNA-PKcs to sites of DNA damage. Nature. 2005; 434:605–611. [PubMed: 15758953]
6. Carney JP, et al. The hMre11/hRad50 protein complex and Nijmegen breakage syndrome: linkage of double-strand break repair to the cellular DNA damage response. Cell. 1998; 93:477–486. [PubMed: 9590181]
7. Maser RS, Zinkel R, Petrini JHJ. An alternative mode of translation permits production of a variant NBS1 protein from the common Nijmegen breakage syndrome allele. Nature Genet. 2001; 27:417–421. [PubMed: 11279524]
8. Maser RS, et al. The MRE11 complex and DNA replication: linkage to E2F and sites of DNA synthesis. Mol Cell Biol. 2001; 21:6006–6016. [PubMed: 11486038]
9. Williams BR, et al. A murine model of Nijmegen breakage syndrome. Curr Biol. 2002; 12:648–653. [PubMed: 11967151]
10. Kang J, Bronson RT, Xu Y. Targeted disruption of NBS1 reveals its roles in mouse development and DNA repair. EMBO J. 2002; 21:1447–1455. [PubMed: 11889050]
11. Difilippantonio S, et al. Role of Nbs1 in the activation of the Atm kinase revealed in humanized mouse models. Nature Cell Biol. 2005; 7:675–685. [PubMed: 15965469]
12. Barlow C, et al. *Atm*-deficient mice: a paradigm of ataxia telangiectasia. Cell. 1996; 86:159–171. [PubMed: 8689683]
13. Xu Y, Baltimore D. Dual roles of ATM in the cellular response to radiation and in cell growth control. Genes Dev. 1996; 10:2401–2410. [PubMed: 8843193]
14. Xu Y, et al. Targeted disruption of ATM leads to growth retardation, chromosomal fragmentation during meiosis, immune defects, and thymic lymphoma. Genes Dev. 1996; 10:2411–2422. [PubMed: 8843194]
15. Yamazaki V, Wegner RD, Kirchgessner CU. Characterization of cell cycle checkpoint responses after ionizing radiation in Nijmegen breakage syndrome cells. Cancer Res. 1998; 58:2316–2322. [PubMed: 9622065]
16. Kang J, et al. Functional interaction of H2AX, NBS1, and p53 in ATM-dependent DNA damage responses and tumor suppression. Mol Cell Biol. 2005; 25:661–670. [PubMed: 15632067]
17. Kang J, Bronson R, Xu Y. Targeted disruption of NBS1 reveals its roles in mouse development and DNA repair. EMBO J. 2002; 21:1447–1455. [PubMed: 11889050]
18. Kitagawa R, Bakkenist CJ, McKinnon PJ, Kastan MB. Phosphorylation of SMC1 is a critical downstream event in the ATM–NBS1–BRCA1 pathway. Genes Dev. 2004; 18:1423–1438. [PubMed: 15175241]
19. Bakkenist CJ, Kastan MB. DNA damage activates ATM through intermolecular autophosphorylation and dimer dissociation. Nature. 2003; 421:499–506. [PubMed: 12556884]
20. Bender CF, et al. Cancer predisposition and hematopoietic failure in *Rad50*$^{S/S}$ mice. Genes Dev. 2002; 16:2237–2251. [PubMed: 12208847]
21. Takai H, et al. Chk2-deficient mice exhibit radioresistance and defective p53-mediated transcription. EMBO J. 2002; 21:5195–5205. [PubMed: 12356735]
22. Hirao A, et al. Chk2 is a tumor suppressor that regulates apoptosis in both an ataxia telangiectasia mutated (ATM)-dependent and an ATM-independent manner. Mol Cell Biol. 2002; 22:6521–6532. [PubMed: 12192050]
23. Falck J, Petrini JH, Williams BR, Lukas J, Bartek J. The DNA damage-dependent intra–S phase checkpoint is regulated by parallel pathways. Nature Genet. 2002; 30:290–294. [PubMed: 11850621]
24. Kamer I, et al. Proapoptotic BID is an ATM effector in the DNA-damage response. Cell. 2005; 122:593–603. [PubMed: 16122426]

25. Zinkel SS, et al. A role for proapoptotic BID in the DNA-damage response. Cell. 2005; 122:579–591. [PubMed: 16122425]

26. Kastan MB, et al. A mammalian cell cycle checkpoint pathway utilizing p53 and *GADD45* is defective in ataxia-telangiectasia. Cell. 1992; 71:587–597. [PubMed: 1423616]

27. Lee JH, Paull TT. ATM activation by DNA double-strand breaks through the Mre11–Rad50–Nbs1 complex. Science. 2005; 308:551–554. [PubMed: 15790808]

28. Theunissen JW, Petrini JH. Methods for studying the cellular response to DNA damage: influence of the Mre11 complex on chromosome metabolism. Methods Enzymol. 2006; 409:251–284. [PubMed: 16793406]

29. Theunissen JW, et al. Checkpoint failure and chromosomal instability without lymphomagenesis in $Mre11^{ATLD1/ATLD1}$ mice. Mol Cell. 2003; 12:1511–1523. [PubMed: 14690604]

30. Liu P, Jenkins NA, Copeland NG. A highly efficient recombineering-based method for generating conditional knockout mutations. Genome Res. 2003; 13:476–484. [PubMed: 12618378]

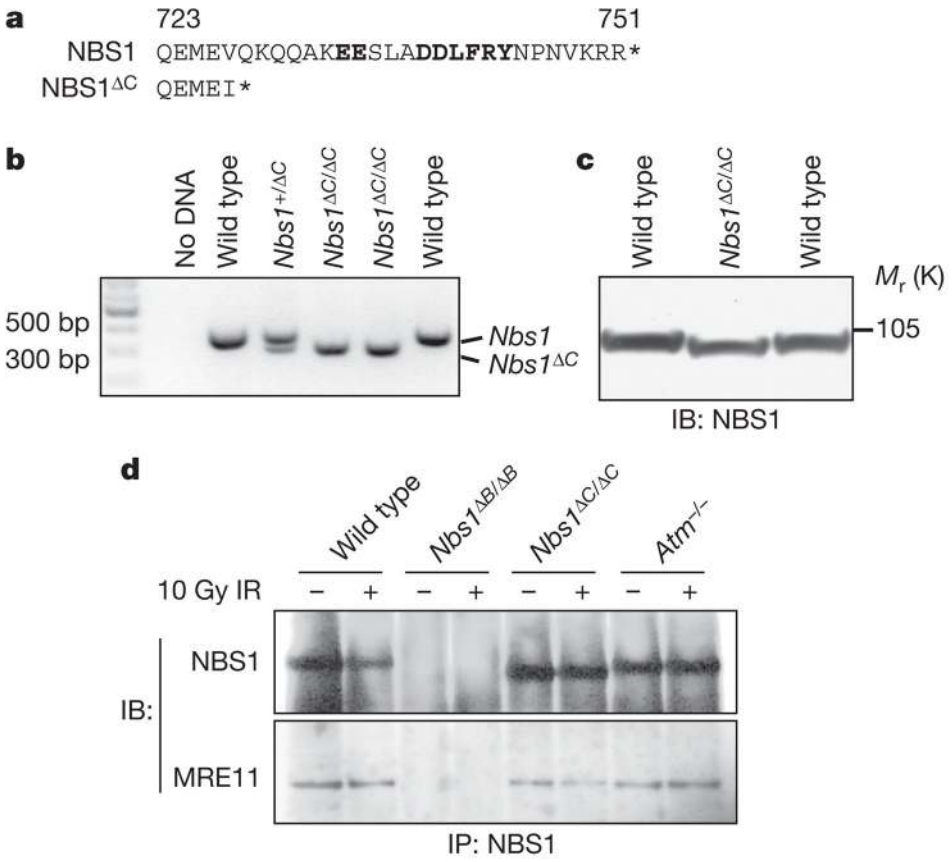


**Figure 1. Generation of *Nbs1*$^{\Delta C/\Delta C}$ mice**

**a**, The C-terminal sequence of NBS1$^{\Delta C}$ is shown compared with wild-type NBS1 (conserved residues in bold)[4,5]. **b**, PCR analysis and sequencing of complementary DNA confirmed splicing from exon 14 to 16 and a nonsense mutation that results in the truncation of the 24 C-terminal amino acids. **c**, Immunoblotting (IB) showed increased mobility of NBS1$^{\Delta C}$ in *Nbs1*$^{\Delta C/\Delta C}$ MEFs.

**d**, Immunoprecipitation (IP) of NBS1 and IB for NBS1 (top) and MRE11 (bottom) from MEFs of the indicated genotype. IR, ionizing radiation.

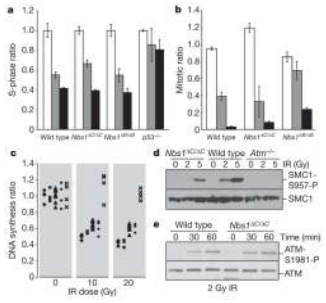

**Figure 2. Cellular phenotypes of *Nbs1*$^{\Delta C/\Delta C}$**

**a**, G1/S checkpoint analysis in MEFs of the indicated genotype. Cells were mock (white), 5 Gy IR (grey) or 10 Gy IR (black) -treated ($n$ = 3; error bars, s.d.). **b**, G2/M checkpoint analysis in MEFs of the indicated genotype. Cells were mock (white), 2 Gy IR (grey) or 10 Gy IR (black) -treated ($n$ = 3; error bars, s.d.). **c**, Intra-S-phase checkpoint in wild-type (diamond), *Nbs1*$^{+/\Delta C}$ (square), *Nbs1*$^{\Delta C/\Delta C}$ (triangle), *Nbs1*$^{\Delta B/\Delta B}$ (circle) or *Atm*$^{-/-}$(cross) MEFs. **d**, IB of SMC1-S957-p and SMC1, in MEFs of the indicated genotype. **e**, IB of ATM-S1981-p and ATM in MEFs after IR treatment.

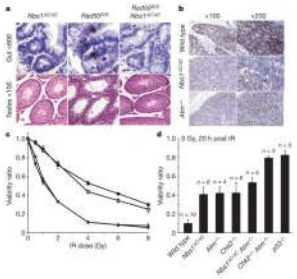

**Figure 3. Apoptotic phenotypes of *Nbs1*$^{\Delta C/\Delta C}$**

**a**, Representative TUNEL stained sections of small intestines from the indicated genotype (top). Haematoxylin and eosin (H&E)-stained sections of testes (bottom). **b**, Cleaved caspase-3 staining of thymi post IR treatment. **c**, Dose response of thymocytes post IR treatment. Triplicate results from 2 *Nbs1*$^{\Delta C/\Delta C}$ (open and closed squares) and 2 *wild type* (open and closed diamonds) animals are shown ($n$ = 3, error bar = s.d.). **d**, Thymocyte apoptosis in the indicated genotypes ($n$, number of animals; error bar, s.d. of triplicate results). $P$-values (Wilcoxon rank sum test) are: $P$(*Nbs1*$^{\Delta C/\Delta C}$ versus wild type) = $2.96 \times 10^{-7}$; $P$(*Nbs1*$^{\Delta C/\Delta C}$ versus *Atm*$^{-/-}$) = 0.35; and $P$(*Nbs1*$^{\Delta C/\Delta C}$ vs. *Nbs1*$^{\Delta C/\Delta C}$ *Atm*$^{-/-}$) = $2.311 \times 10^{-5}$.

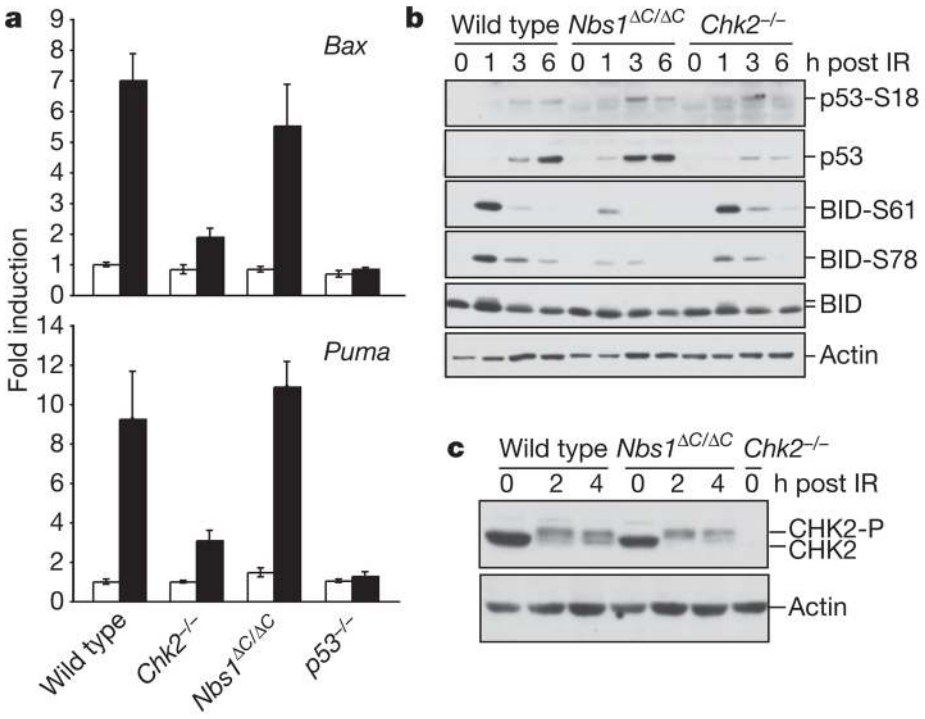


**Figure 4. Apoptotic signalling in *Nbs1*$^{\Delta C/\Delta C}$**

**a**, Quantitative PCR analysis of p53-dependent proapoptotic genes. Induction of *Bax* and *Puma* from a representative experiment performed in triplicate is shown (error bars, s.d.). Mock-treated (white) or IR-treated (black) thymocytes, 8 h post 5 Gy IR. **b**, Western blot analysis of p53-S18, p53, phosphorylated BID (S61, S78), BID, and actin in thymocytes after 5 Gy of IR at the indicated times post treatment. **c**, Western blot analysis of CHK2 hyperphosphorylation in thymocytes at the indicated times post 5 Gy IR.